

Evidence for a direct role of the disease modifier SCNM1 in splicing

Viive M. Howell, Julie M. Jones, Sarah K. Bergren, Li Li, Allison C. Billi, Matthew R. Avenarius and Miriam H. Meisler*

Department of Human Genetics, University of Michigan School of Medicine, Ann Arbor, MI 48109-0618, USA

Received July 9, 2007; Revised July 9, 2007; Accepted July 22, 2007

We originally isolated *Scnm1* as a disease modifier gene that is required for efficient *in vivo* splicing of a mutant splice donor site in the sodium channel *Scn8a*. It was previously unclear whether the modifier effect on splicing was direct or indirect. We now report evidence that sodium channel modifier 1 (SCNM1) has a direct role in splicing. SCNM1 protein interacts with the spliceosome protein U1-70K in the yeast two-hybrid system, and is co-localized with U1-70K in nuclear speckles in mammalian cells. SCNM1 is also co-immunoprecipitated with the spliceosomal core Smith (Sm) proteins and demonstrates functional activity in a minigene splicing assay. In a yeast two-hybrid screen, SCNM1 interacted with LUC7L2, a mammalian homolog of a yeast protein involved in recognition of non-consensus splice donor sites. This interaction requires the acidic C-terminal domain of SCNM1 which is truncated by the disease susceptibility variant *Scnm1*^{R187X} in mouse strain C57BL/6J. *Luc7L2* transcripts are widely distributed in mammalian tissues, and undergo alternative splicing and polyadenylation. LUC7L2 is also co-localized with U1-70K and may function with SCNM1 in recognition of weak splice donor sites. In summary, *Scnm1* is the first example of a modifier gene which influences disease severity through a *trans*-effect on splicing of the disease gene transcript.

INTRODUCTION

Scnm1 was originally discovered as a genetic modifier of a disorder caused by mutation of a splice donor site in the sodium channel gene *Scn8a* (1). The mutant donor site, GAgtaaca, contains a C nucleotide in place of the consensus G at the +5 position of the intron. Compared with wildtype *Scnm1*, the variant *Scnm1*^{R187X} in mouse strain C57BL/6J reduces splicing of the non-consensus donor site from 10% to 5% of transcripts, bringing the level of functional sodium channel below the minimum required for survival (1,2). *Scnm1*^{R187X} is thus an example of naturally occurring disease susceptibility variant, whose deleterious effect is only apparent in the presence of mutation at another locus. Both the lethal disorder and the splicing deficiency are corrected by expression of wild type *Scnm1* as a transgene (1).

The 229 amino acid sodium channel modifier 1 (SCNM1) protein contains an N-terminal bipartite nuclear localization signal, an acidic C-terminal domain, and a C2H2 zinc finger whose sequence is related to the U1 family of splice factors

involved in exon recognition (1). The *Scnm1* transcript is ubiquitously expressed in mammalian tissues, consistent with a role in basic cell biology.

The *in vivo* effect on splicing and the phylogenetic relationship of its zinc finger domain to the U1 proteins suggested that SCNM1 may itself be a spliceosome component with a direct role in donor site recognition (1). However, proteomic analyses of mammalian spliceosomes have not detected SCNM1 as a core spliceosomal component (3). Previous data did not eliminate the possibility that the *in vivo* effect of SCNM1 on splicing was mediated by an indirect mechanism. To further address this question, we have characterized the subnuclear localization of SCNM1, carried out a yeast two-hybrid screen for interacting proteins, and developed a minigene assay for splicing activity.

Spliceosomal proteins are characterized by non-uniform distribution within the nucleus, concentrated in aggregates called 'speckles'. Some diffuse nuclear distribution may also be evident (4,5). Distribution between these sites may be mediated by protein phosphorylation, and speckles could represent storage sites for inactive proteins (6,7). Various protein

*To whom correspondence should be addressed. Tel: +734 763 5546; Fax: +734 763 9691; Email: meislerm@umich.edu

components of the spliceosome have distinct but overlapping distributions in these two compartments (7–10).

The data reported here support the model that SCNM1 is co-localized with spliceosomal proteins and may have a direct role in recognition of non-consensus donor sites. We also report interaction with LUC7L2, the mammalian homolog of Luc7p, a protein required for recognition of non-consensus splice donor sites in yeast (11).

RESULTS

SCNM1 interacts with the spliceosome component U1-70K

To identify proteins that interact with SCNM1, we carried out a yeast two-hybrid screen using the fusion protein LexA–SCNM1 as bait. Clones (3×10^7) from a mouse embryonic cDNA library were screened by large-scale transformation. Two strongly positive clones, y1 and y2, were isolated. The inserts contain overlapping fragments of the spliceosomal protein U1-70K, a component of the U1 snRNP. The inserts include part of the N-terminal domain that interacts with the U1snRNP and the RNA recognition motif (RRM) (Fig. 1A). Interaction with U1-70K suggests that SCNM1 could be a component of the spliceosome.

Generation of an antiserum to SCNM1

HIS-tagged bacterially expressed full-length SCNM1 was isolated as described in Methods and used to generate a rabbit polyclonal antiserum. On western blots, the antiserum recognized the wildtype 229 residue SCNM1 protein from mouse strain C3H (Fig. 1B). The *Scnm1*^{R187X} allele in strain C57BL/6J is predicted to generate two mutant proteins of 164 and 187 residues (1), and both were detected by western blot (Fig. 1B). Immunostaining of cultured 293T cells with affinity-purified antiserum revealed a non-uniform nuclear distribution of endogenous SCNM1 (Fig. 1C). Co-staining with anti-SCNM1 and anti-U1-70K produced overlapping patterns of immunofluorescence, indicative of partial co-localization of the endogenous proteins (Fig. 1C).

The Sm antiserum Y12 recognizes core Sm spliceosomal proteins B'/B and D which contain a symmetrical dimethylarginine motif (4,12). Lysates of 293T cell were immunoprecipitated with anti-Sm, and a western blot of the Sm and normal mouse IgG immunoprecipitates were probed with anti-SCNM1. (In this experiment, purified IgG was used for pre-clearing of lysates.) SCNM1 protein was present in the Sm immunoprecipitate but not in the non-specific IgG precipitate (Fig. 1D). Immunofluorescent analysis of 293T cells stained with anti-SCNM1 and anti-Sm revealed co-localization of the endogenous proteins (Fig. 1E). These results provide further evidence that SCNM1 protein is associated with spliceosomal proteins.

Activity of SCNM1 in a minigene splicing assay

The *Scn8a*–medJ minigene construct containing exons 1–4 is shown in Figure 1F. The minigene contains the medJ mutation in the splice donor site of exon 3 (asterisk) and a unique sequence tag in exon 4 for specific amplification of

the minigene transcript. Because intron 2 of *Scn8a* is a minor class U12 (AT–AC) intron, the exon 3 splice site mutation results in skipping of both exon 2 and exon 3 (1,13). Inclusion of exon 2 and exon 3 is increased by expression of a wildtype SCNM1 transgene in C57BL/6J–medJ brain (1).

Transfection of COS7 cells with the minigene generated a major product of 0.3 kb that skips exon 2 and exon 3, like the major *in vivo* product (1,13), and a minor product of 0.9 kb that contains exon 2 and exon 3 and also retains intron 3 (Fig. 1G). Retention of intron 3 is not seen *in vivo*, and reflects a limitation of the COS7 cell system. The minor product containing exon 2 and exon 3 accounts for 28% of minigene transcripts, based on quantitation of FAM-labeled transcripts (Fig. 1H, control). Co-transfection of *Scnm1* cDNA with the minigene resulted in a significant increase in the proportion of transcripts containing exon 2 and exon 3, from 28% to 41% (Fig. 1G and H). This change is greater than the 5% increase that results from expression of the *Scnm1* transgene in C57BL/6J–medJ mice (1), and demonstrates a direct effect of SCNM1 on splicing of the medJ transcript.

Identification of a novel protein that interacts with SCNM1

Inserts were isolated from 286 strongly positive colonies from the yeast two-hybrid screen and digested with the restriction endonuclease *AluI*. More than 60% of the positive clones contained the same set of *AluI* fragments (Fig. 2A). The 0.5 kb insert for several of these clones, including clone y3, were sequenced and found to match the predicted gene *Luc7L2* (*NM_138680.1*, NP_619621.1). The insert encodes an internal fragment of the LUC7L2 protein with 166 amino acids that includes part of the coiled-coil domain, the second zinc finger, the RE domain, and part of the RS domain (Fig. 2B and C). Three nuclear localization signals are included (Fig. 2C, asterisk).

Comparison of the cDNA sequences with the mouse genome sequence (build 36.1) located the *Luc7L2* gene on mouse chromosome 6 at a position 38.5 Mb from the centromere. The human ortholog is located on chromosome 7q34 at 138.7 Mb (human genome build 36.2). Mammalian LUC7L2 exhibits 30% amino acid sequence identity to yeast Luc7p, a spliceosomal protein involved in recognition of weak splice donor sites (11) (Fig. 2C). There are two other homologs of Luc7p in the mammalian genome, the spliceosomal protein CROP/LUC7LA and the myogenic protein LUC7L (Fig. 2C). Both CROP and LUC7L have been localized to nuclear speckles (14,15).

To determine whether SCNM1 can interact with these homologs, we synthesized VP16 fusion constructs containing fragments of CROP and LUC7L corresponding to the domains of LUC7L2 present in the y3 clone. The CROP and LUC7L constructs were tested in the yeast two-hybrid system by co-transformation with pLexA–SCNM1. Only weak interaction was observed with LUC7L, and no interaction was observed with CROP, demonstrating preferential interaction of SCNM1 with LUC7L2 (data not shown).

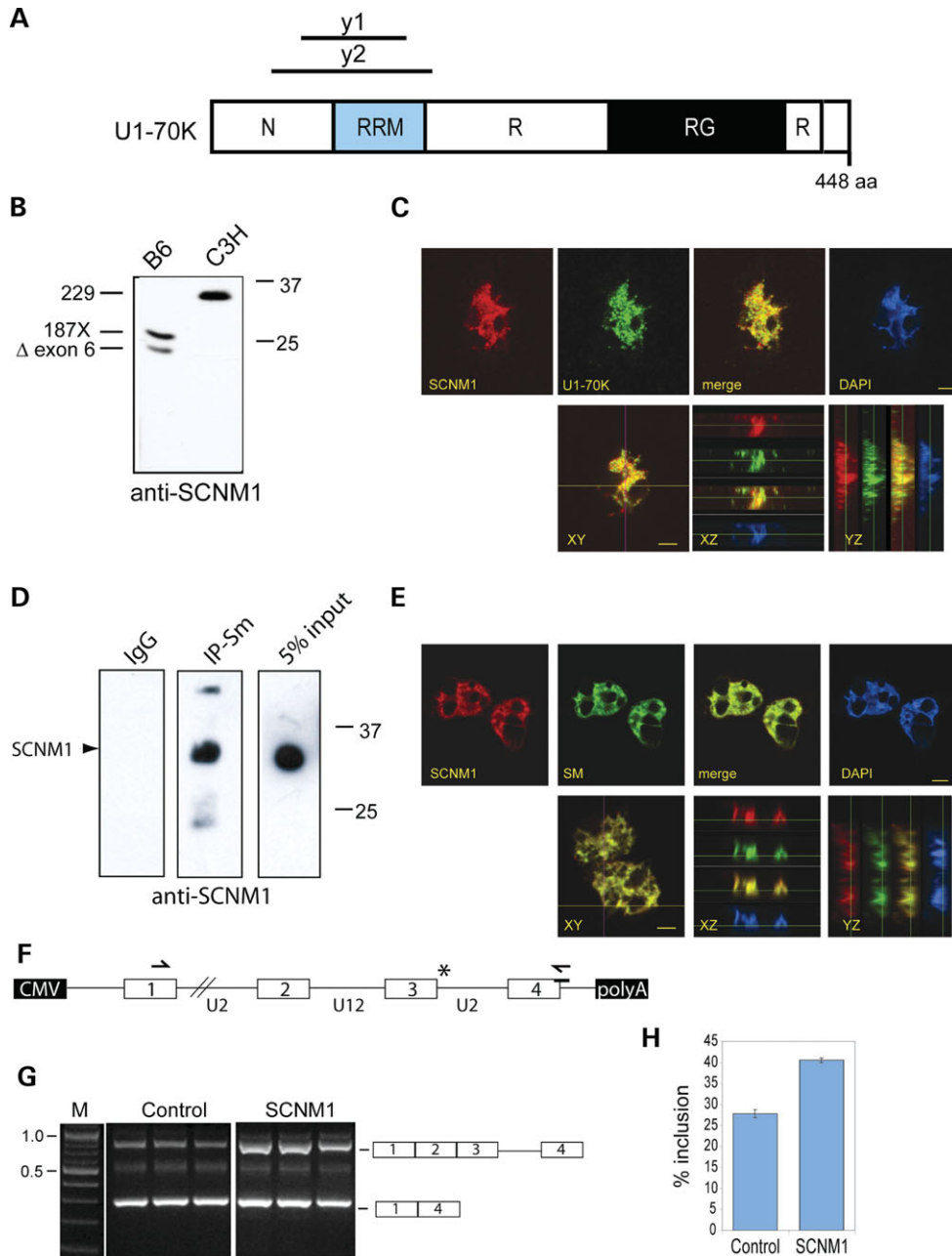


Figure 1. SCNM1 interacts with U1-70K and Sm proteins. (A) Two cDNA clones that were strongly positive in the yeast two-hybrid screen, y1 and y2, encode overlapping fragments of U1-70K. The domain structure of the 448 residue U1-70K protein is shown. N, N-terminal domain (involved in protein–protein interactions); RRM, RNA recognition motif; R, arginine-rich region; RG, arginine–glycine rich region. (B) Western blot of endogenous SCNM1 detected with affinity-purified anti-SCNM1 (1 : 500) in 50 µg nuclear extracts from testis of mouse strains C57BL/6J (B6) and C3HeB/FeJ (C3H). C3H mice produce the full-length protein of 229 amino acids, whereas B6 mice are homozygous for *Scnm1*^{R187X} which encodes two mutant proteins, 187X (186 residues) and Δ exon 6 (164 residues). The SCNM1 proteins migrate to a position 5 kDa larger than their predicted molecular weights. Molecular weight markers in kDa at right. (C) Fluorescent 0.5 µm confocal images of 293T cells immunostained for endogenous SCNM1 (red), and U1-70K (green). Both proteins exhibit a speckled subnuclear distribution. XY, XZ and YZ are multiplane views of the Z stack projection. Lines on the XY merged projection image indicate the axis position of the rotated transverse (vertical: YZ) and cross-section (horizontal: XZ) images through the Z stack. Regions of co-localization of the two proteins are visible in the merged image (yellow). Nuclei were visualized with DAPI (blue). Bar: 5 µm. (D) Immunoprecipitation of SCNM1 by anti-Sm (Y12) from nuclear extracts of 293T cells. The Sm immunoprecipitate (IP-Sm), but not the mouse IgG immunoprecipitate (IgG: negative control) contains SCNM1, detected on the western blot with anti-SCNM1. SCNM1 is also detected in 5% of non-immunoprecipitated nuclear extract (5% input). (E) Immunofluorescence 0.5 µm confocal image of 293T cells stained for endogenous SCNM1 (red) and Sm (green). XY, YZ and XZ are confocal multiplane views of a Z stack projection as described in Fig 1B. Regions of co-localization of the two proteins are visible in the merged image (yellow). Cells were counterstained with DAPI (blue) to visualise the nucleus. Both proteins exhibit a punctate sub-nuclear localization. Bar: 5 µm. (F) The structure of the *Scn8a* minigene containing the medJ mutation in the splice donor site of exon 3 (*) and a unique sequence tag in exon 4. (G) COS7 cells were co-transfected with 0.3 µg of *Scn8a* minigene and 2 µg of *Scnm1* cDNA or empty vector (control). RT-PCR products were amplified with a forward primer in exon 1 and reverse primer in the exon 4 tag. Products were isolated from ethidium bromide-stained gels and sequenced. (H) Quantitation of the minigene assay. RT-PCR products were separated by capillary electrophoresis and the FAM-label from the primer was quantitated using Genemapper software. Percentage of transcript containing exon 2 and exon 3, mean + / - SD.

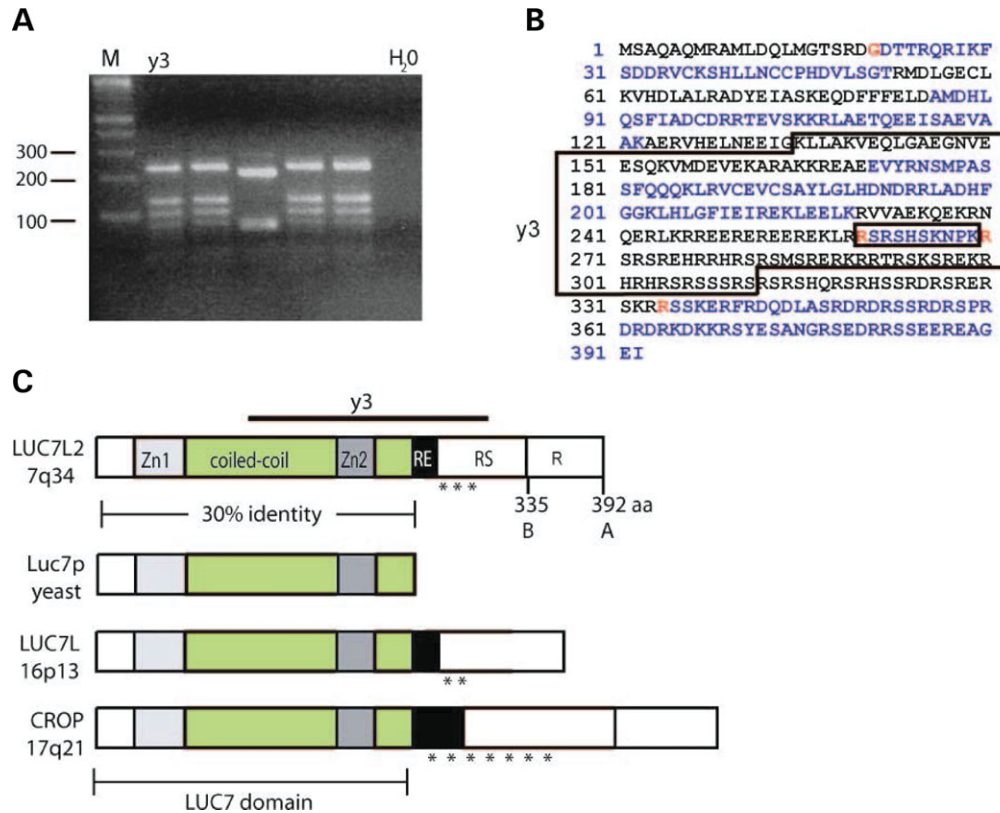


Figure 2. Identification of the LUC7L2 clone. (A) Agarose gel electrophoresis of *AluI* digested inserts from five cDNA clones that were strongly positive for interaction with SCNM1 in the yeast two-hybrid system. Four of the five clones contain identical *AluI* fragments. M, molecular weight marker (bp). (B) Amino acid sequence of clone y3 (boxed) matches LUC7L2 (NP_619621.1). Alternating exons are shown in blue and black; residues that span exon junctions are shown in red. The small inner box represents exon 8, which is alternatively spliced and is not present in clone y3. (C) The predicted domain structure of the 392-residue LUC7L2 protein. Zn1, CCCH zinc finger; green, coiled-coil regions; Zn2, C2H2 zinc finger; RE, arginine, glutamate-rich region; RS, arginine, serine-rich region; R, arginine-rich region; asterisk, nuclear localization signal. Mammalian LUC7L2 exhibits 30% overall amino acid sequence identity to yeast Luc7p. The structures of the mammalian paralogs LUC7L and LUC7LA/CROP are indicated. Alternatively spliced forms of both paralogs have been described. The chromosomal locations of the human genes are indicated.

Interaction domains of SCNM1 and LUC7L2

The interaction between LUC7L2 clone y3 and wildtype SCNM1 was further examined in a yeast mating assay. Strong interaction was confirmed by growth in selective media in the presence of 3 mM 3-amino triazole and by intense *LacZ* staining (Fig. 3A). We used this assay to test the interaction of LUC7L2 with the two mutated SCNM1 proteins from strain C57BL/6J. Deletion of the acidic C-terminus in the 187X truncated protein abolished interaction with LUC7L2, but the internal deletion of exon 6 had no effect (Fig. 3A). Since the major SCNM1 protein in tissues from C57BL/6J mice is 187X (Fig. 1B), impaired binding of LUC7L2 could contribute to the deficiency in splicing of the *Scn8a^{medJ}* transcript in these mice.

The LUC7L2 clone y3 contains two arginine-rich basic domains (RE and RS, Fig. 2C) which could interact with the acidic domain of SCNM1. The RS domain is thought to mediate protein localization to nuclear speckles (16). To determine whether the RS domain is sufficient for interaction with SCNM1, we generated a construct encoding 109 amino acids that includes the RS domain. This fragment did not interact with full-length SCNM1 (Fig. 3B).

Alternative polyadenylation of *Luc7L2* transcripts and alternative splicing of exon 8

A northern blot containing 2 μ g of poly(A)⁺ RNA from brain was hybridized with a cDNA probe containing coding sequences from exons 9 and 10 of *Luc7L2*. Two major transcripts were detected, a short transcript of 2.9 kb (transcript A) and a long transcript of 5.7 kb (transcript B) (Fig. 4A, lane 1). In addition to brain, transcripts A and B are also present in kidney, heart, thymus, stomach, skeletal muscle and testis (data not shown).

A probe complementary to 3'-UTR sequence downstream of the translation termination codon in exon 10 (Fig. 4C probe 2) hybridized specifically to the 2.7 kb transcript A (Fig. 4A, lane 2). This transcript thus contains exon 10 and encodes the full length 392 residue LUC7L2 protein.

To identify the 3'-UTR of transcript B, we examined *Luc7L2* cDNA clones in sequence databases. The 4.2 kb cDNA clone BC056383 contains exons 1–9 and extends through the splice donor site of exon 9 to terminate at a polyadenylation site 2.9 kb downstream (Fig. 4C). The open reading frame of transcript B contains one tyrosine codon downstream of exon 9, encoding a 335 residue protein. A probe containing 455 bp

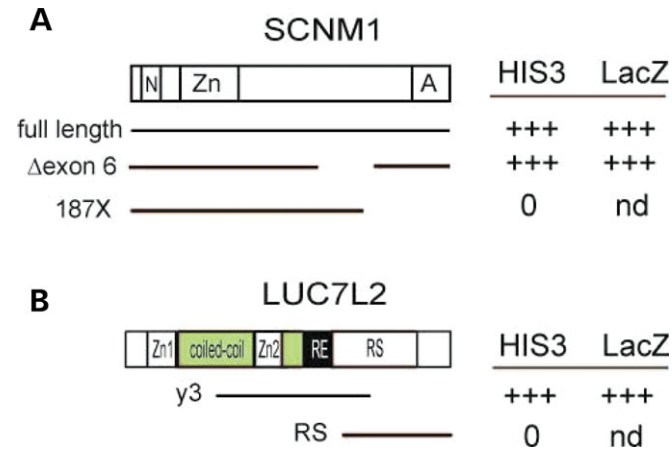


Figure 3. Interaction of SCNM1 and LUC7L2 in the yeast two-hybrid assay. (A) The SCNM1 protein contains a nuclear localization signal (N), a C2H2 zinc finger (Zn) and an acidic C-terminal domain (A). Three SCNM1 clones used as fusion baits are indicated. Results of two-way tests with LUC7L2 clone y3 are indicated. Δ exon 6 and R187X are naturally occurring variants in strain C57BL/6J (1). (B) The domains of the LUC7L2 protein are indicated. The results of the mating assay for interaction between full length SCNM1 and two LUC7L2 cDNA clones are indicated. +++, strongly positive; 0, negative; nd, not done.

from the 2.9 kb 3'-UTR of transcript B (Fig. 4C probe 3) hybridized specifically with transcript B (Fig. 4A, lane 3). The B isoform of LUC7L2 lacks the arginine-rich C-terminal domain (R) encoded by exon 10 (Fig. 2C).

The tissue distribution of transcripts A and B was examined by RT-PCR. Transcript A was amplified with a forward primer in exon 7 and a reverse primer in the 3'-UTR from exon 10. Expression was observed in all tissues tested (Fig. 4B). Unexpectedly, two RT-PCR products were amplified with these primers. Sequencing demonstrated that the shorter product lacks the 30 bp exon 8, which encodes amino acid residues 260–269 of LUC7L2 at the 5' end of the RS-rich region (Fig. 2B, small box). RT-PCR of transcript B with a forward primer in exon 7 and reverse primer in intron 9 also amplified two products, one with and another without exon 8 (Fig. 4B). Thus, the choice of polyadenylation site and the alternate splicing of exon 8 do not demonstrate tissue-specificity.

Large-scale expression data for *Luc7L2* from EST and microarray databases

The results of two large-scale expression studies extend our analysis of *Luc7L2* to additional tissues. The expression profile from Unigene Mm.276133, based on EST frequencies in tissue-specific libraries, demonstrates abundant expression in many adult tissues and during embryonic development. The highest frequency of *Luc7L2* clones was observed in lymph node (>0.5 transcripts per million), sympathetic ganglia (>0.5 transcripts per million), and mid-gestation embryo (>0.1 transcripts per million) (<http://www.ncbi.nlm.nih.gov/UniGene>). Using the Affymetrix GNF1M expression microarrays, expression was detected in all of the RNA samples from 61 mouse tissues (<http://symatlas.gnf.org>).

Co-localization of LUC7L2 with the spliceosome marker U1-70K

The subcellular localization of LUC7L2 was investigated using an EGFP-tagged LUC7L2 fusion construct containing exon 10 and lacking exon 8. The construct was transiently transfected into 293T cells and protein expression was examined by confocal microscopy. EGFP-LUC7L2 was localized exclusively to the nucleus, and exhibited a predominantly speckled distribution (Fig. 5A). The same cDNA construct fused to MYC showed similar distribution (data not shown). A myc-tagged fusion protein constructed from clone y3 also exhibited a speckled distribution, indicating that a portion of the RS domain is sufficient for localization (data not shown).

Co-transfection of the EGFP-LUC7L2 construct with MYC-U1-70K revealed co-localization of LUC7L2 and U1-70K in nuclear speckles as well as diffuse staining for both proteins in the nucleoplasm (Fig. 5B).

Co-localization of SCNM1 and LUC7L2

To confirm the interaction between SCNM1 and LUC7L2 observed in yeast, we transfected full length SCNM1 and MYC-LUC7L2 (with exon 10, lacking exon 8) into 293T cells. Both proteins were localized to the nucleus. Partial co-localization was indicated by overlapping (yellow) fluorescence (Fig. 5C). This result confirms the co-localization of these proteins, both of which interact with U1-70K.

The activity of LUC7L2 in the *Scn8a* minigene splicing assay was tested as described in Figure 1F to H. Transfection of LUC7L2 cDNA with the minigene did not increase the inclusion of exons 2 and 3 (Fig. 4D). When LUC7L2 cDNA was combined with SCNM1 cDNA (Fig. 4D, L + S), the effect was no greater than that described above for SCNM1 alone. Since COS7 cells express endogenous *Scnm1* and *Luc7L2* (SB and MM, data not shown), there may be an excess of LUC7L2 in the cells which masks the effect of the exogenous protein in this assay.

DISCUSSION

The deleterious effect of the *Scnm1*^{R187X} variant on survival of medJ mice with a splice site mutation in sodium channel *Scn8a* is mediated by impaired splicing of the medJ mutant transcript *in vivo* (1). The interaction of SCNM1 with the spliceosomal protein U1-70K, and its functional activity in the medJ minigene assay, suggest that the *in vivo* effect results from a direct role of SCNM1 in splicing. The interaction of LUC7L2 with SCNM1 and U1-70K indicate that both SCNM1 and LUC7L2 are associated with the U1 snRNP spliceosomal subunit. We suggest that SCNM1 and LUC7L2 have an auxiliary role in splicing through stabilization of the spliceosome/pre-mRNA complex at non-consensus splice donor sites. A model depicting these interactions is presented in Figure 6.

The absence of SCNM1 and LUC7L2 from proteomic analyses of purified spliceosomes (3) may be accounted for if their association with the spliceosome is transient, or if they are associated with a minor population of spliceosomes. In a

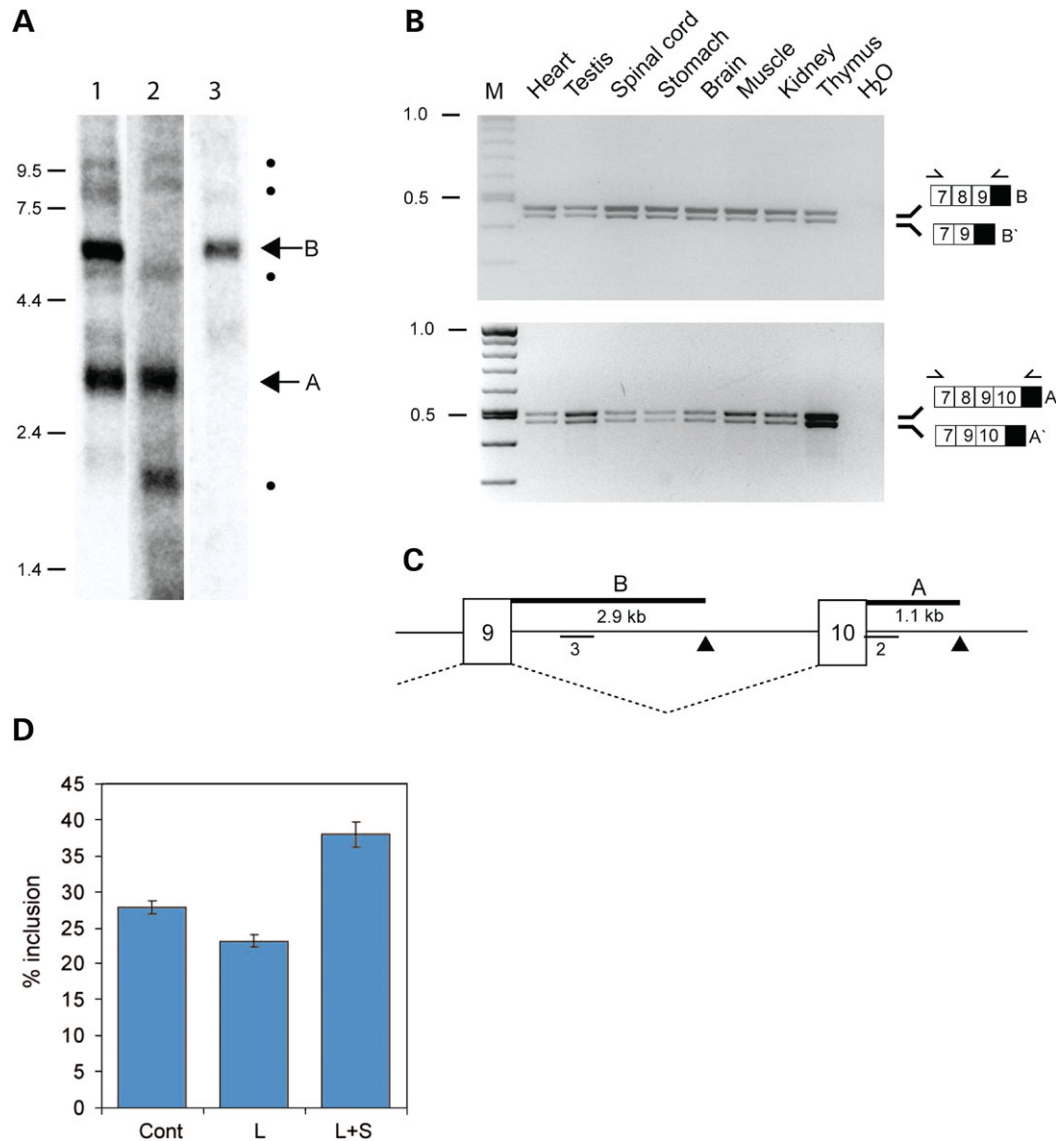


Figure 4. Expression and alternative splicing of *Luc7L2*. (A) Northern blot containing 2 μ g of poly(A)⁺RNA from B6 mouse brain. Lanes were separately hybridized with three cDNA probes. Lane 1, 0.4 kb cDNA probe containing coding sequence from exon 9 and exon 10. Two major transcripts are detected, A (2.9 kb) and B (5.7 kb). Minor bands are also indicated (filled circle). Lane 2, 0.6 kb cDNA probe from the 3'-UTR in exon 10 hybridizes with transcript A but not transcript B. Lane 3, 0.4 kb cDNA probe from the 3'-UTR downstream of exon 9 hybridizes with transcript B. (B) RT-PCR of RNA from C57BL/6J mouse tissues. Transcripts B and A were amplified with different reverse primers. Both transcripts exhibit alternative splicing of exon 8. M, molecular weight markers (kb). (C) The A and B transcripts of *Luc7L2* differ in their C-terminus and 3'-UTR due to use of alternative polyadenylation sites (triangles). The 3'-UTR probes used in lanes 2 and 3 of the northern blot are indicated. (D) Minigene assay results showing the percentage of transcript containing exon 2 and exon 3, mean \pm SD. Cont, control with empty vector; L, *Luc7L2* cDNA; L + S, *Luc7L2* cDNA plus *Scnm1* cDNA.

similar example, the auxiliary factor TIA1 is thought to interact with U1C to stabilize weak splice donor sites (17), but TIA1 is not detected in purified mammalian spliceosomes under standard conditions (3). TIA1 interacts with the zinc finger domain of U1C, which also mediates interaction of U1C with U1-70K and integration of U1C into the U1snRNP (18). The interaction of SCNM1 with LUC7L2 is mediated by the acidic domain of SCNM1 and does not require the zinc-finger domain. A transient association of LUC7L2 and SCNM1 with the U1 snRNP may stabilize the spliceosome and increase splicing efficiency. SCNM1 does

not contain an RRM domain and is therefore unlikely to interact directly with pre-mRNA, although the U1-type zinc finger could mediate interaction with RNA (19).

Using a rabbit SCNM1 antiserum, we were able to detect the two predicted protein products of the *Scnm1*^{R187X} variant (1). The major protein, 187X, lacks the acidic C-terminal domain that is required for interaction with LUC7L2, which could contribute to the impaired *in vivo* function. *Luc7p* is a component of the yeast U1snRNP that was identified in a genetic screen of genes affecting the cap-binding complex (CBC) of *Saccharomyces cerevisiae*, the first protein

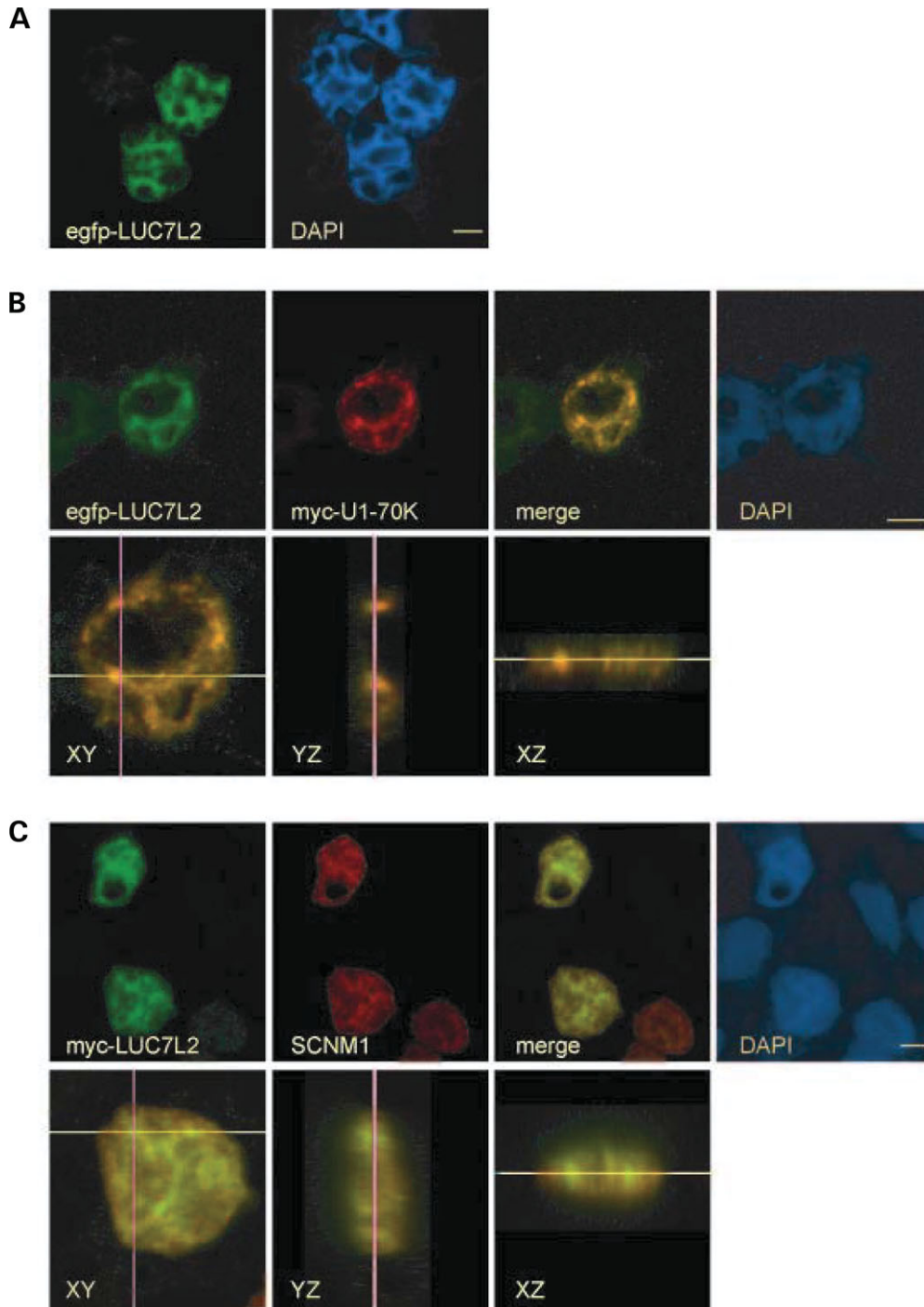


Figure 5. Subcellular localization of LUC7L2 in nuclear speckles and colocalization with U1-70K and SCNM1. (A) Fluorescent 0.4 μm confocal image of EGFP-LUC7L2 (green) in transfected 293T cells. Cells were counterstained with DAPI (blue) to define the nucleus; bar: 5 μm . (B) Fluorescent 0.4 μm confocal image of EGFP-LUC7L2 (green) and MYC-U1-70K (red), in co-transfected 293T cells. Co-localization of the two proteins (yellow) is shown in the merged image. XY, YZ and XZ are zoomed and merged confocal multiplane views of the Z stack projection (described in Fig. 1). (C) Fluorescent confocal Z stack projection and multiplane views of MYC-LUC7L2 (green) detected by anti-MYC, and SCNM1 (red) detected by anti-SCNM1, in co-transfected 293T cells. Co-localization of the two proteins (yellow) is shown in the merged images.

complex to assemble on the pre-mRNA (11,20). Mutations of *LUC7* result in lethality in the absence of CBC, hence the name ‘Lethal Unless CBC is produced’ (21). Mutation of *LUC7* reduced the splicing efficiency of the U1 snRNP toward

transcripts with a non-consensus nucleotide at position +5 of the splice donor site (11), similar to the *Scn8a* mutation that led to the discovery of *Scnm1*^{R187X}. If SCNM1 and LUC7L2 function together in recognition of non-consensus sites, then

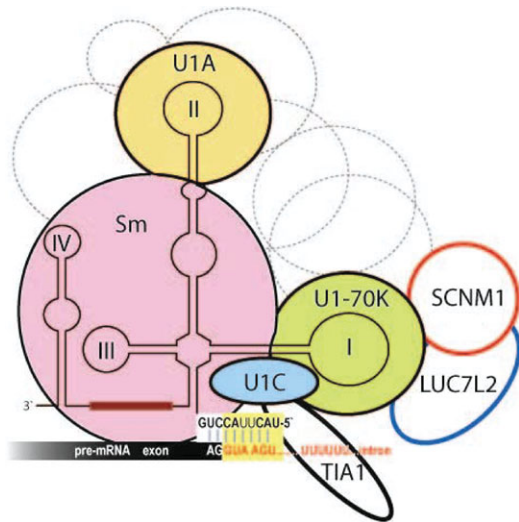


Figure 6. Model for association of SCNMI and LUC7L2 with the mammalian spliceosomal subunit U1 snRNP. We have presented evidence for two-way interactions between SCNMI, LUC7L2 and U1-70K, as indicated in the model. The thin black line represents the secondary structure of the 165 bp U1 snRNA, with stem loops I–IV and a 5' sequence complementary to the splice donor site of pre-mRNA (shaded yellow). The essential protein components of the U1 snRNP include the Sm protein complex which bind nucleotides 126–132 of the U1 snRNA (brown bar), the U1A protein which binds U1 snRNA at stem loop II, the U1-70K protein which binds U1 snRNA at stem loop I, and the U1C protein which interacts with U1-70K and Sm proteins. Additional proteins can associate with the U1 snRNP, including TIA1, which interacts with U1C and binds U-rich intronic regions of pre-mRNAs containing non-consensus splice donor sites (17). Figure adapted from Muto *et al.* (40).

the loss of interaction caused by the *Scnm1*^{R187X} variant may contribute to impaired splicing and disease susceptibility in strain C57BL/6J.

Mammalian LUC7L2 exhibits 30% amino acid sequence identity to Luc7p. Like other mammalian homologs of yeast splice factors, LUC7L2 has acquired an arginine-rich C-terminal domain with an RS region that is thought to direct protein localization to nuclear splicing speckles in a process that is modulated by phosphorylation (6,7,22). We observed co-localization of LUC7L2 with U1-70K in a nuclear speckled distribution. CROP, another mammalian homolog of Luc7p, is also a spliceosomal component (23,24). CROP interacts directly with splice factors SF2/ASF and SRp53 (14,25) and binds the *cis*-acting cAMP regulatory element of the CRH gene (26).

The *Luc7L2* transcript is ubiquitously expressed in mammalian tissues. An alternative polyadenylation site in intron 9 gives rise to two major proteins with different C-terminal domains. *Luc7L* is a paralog of *Luc7L2* with 72% amino acid sequence identity and conservation of alternative polyadenylation, as indicated by the sequences of transcripts *NM_025881* and *NM_028190*. *Luc7L* is expressed in many mouse tissues, and may have a role in regulation of myogenesis (14).

Approximately 15% of human disease mutations are located in splice recognition sites. Clinical severity among patients with identical splice site mutations can vary greatly, as demonstrated most clearly in familial dysautonomia (27) and

cystic fibrosis (28). There is currently considerable interest in developing therapies for disorders affecting splicing. Disease severity in mice with spinal motor atrophy can be improved by administration of sodium butyrate, a histone deacetylase inhibitor that increases inclusion of exon 7 of *SMN2* (29). Other therapeutics being assessed include kinetin, a plant growth hormone (30), the splice factors SC-35, HTRA2-beta1 (31) and TDP43 for cystic fibrosis (32) and spliceosome-mediated RNA *trans*-splicing (33). The genetic factors which influence splicing efficiency in human populations are not known. In a screen of 179 normal individuals we identified several polymorphic variants of *SCNM1* (unpublished data). By analogy with the effect of *Scnm1*^{R187X} in the mouse, these variants could contribute to human disease susceptibility.

MATERIALS AND METHODS

Antibodies

A cDNA fragment encoding the full length SCNMI protein (nucleotides 94–836 in *NM_027013*) was amplified from brain RNA (mouse strain C3HeB/FeJ) and cloned into the *Bam*HI and *Eco*RI sites of expression vector pRSETA (Invitrogen Corporation, Carlsbad, CA, USA), adding a poly-histidine tag (6 X HIS) at the N-terminus of SCNMI. Recombinant protein was expressed in *E. coli* and purified with the Ni-NTA Purification System (Invitrogen Corporation). Rabbit polyclonal antiserum to the purified protein was generated and affinity-purified by Pocono Rabbit Farm and Laboratory, Inc, Canadensis, PA. The antiserum was used at 1 : 100 or 1 : 500 dilution for western blots and immunofluorescence. Mouse monoclonal anti-Sm (Y12) (1 : 250 dilution for immunofluorescence) was a gift from Joan Steitz (4). Mouse monoclonal anti-U1-70K (clone H111) (34), used at 1 : 250 dilution for immunofluorescence, was obtained from Synaptic Systems, Gottingen, Germany. Mouse monoclonal anti-MYC (1 : 2500 dilution) was obtained from Clontech Laboratories Inc., Mountain View, CA, USA. Secondary antibodies anti-rabbit-Alexa Fluor 594 (1 : 800 dilution), anti-mouse-Alexa Fluor 488 (1 : 500 dilution) and anti-mouse Alexa Fluor 594 (1 : 500 dilution) were obtained from Invitrogen Corporation.

Cell culture and transfections

The 293T cell line was grown in Dulbecco's modified Eagle media with high Glucose and L-Glutamine (Invitrogen Corporation) supplemented with 8% bovine serum (Invitrogen Corporation) and incubated at 37°C in the presence of 10% CO₂. 293T cells in 12-well plates were transfected with 70 ng of DNA in 50 μl of 0.25 M CaCl₂ and 50 μl of 2 × HEPES Buffered Phosphate Buffer per well.

COS7 cells for the minigene splicing assay were cultured in Dulbecco's modified Eagle media as described above, supplemented with 10% fetal bovine serum (Invitrogen Corporation) and incubated at 37°C in the presence of 5% CO₂. Cells were plated at a density of 20 × 10⁴ in six well-plates and transfected 12–16 h later with a total of 2.3 μg of endotoxin-free DNA in the presence of 9 μl of Fugene 6

(Roche Diagnostics Corporation, Indianapolis, IN, USA) according to the manufacturer's protocols.

Western blot

Nuclear extracts were prepared from fresh mouse tissue and cells using the CellLytic NuCLEAR Extraction Kit (Sigma-Aldrich, St. Louis, MO, USA) according to the manufacturer's instructions. For western blots, 50 µg of protein was mixed with sample loading dye containing beta-2-mercaptoethanol, incubated at 100°C for 3 min and loaded onto 15% SDS-polyacrylamide minigels. After electrophoresis for 2 h at 175 V, the gels were electroblotted overnight, immunoblotted with anti-SCNM1, and examined by enhanced chemiluminescence using SuperSignal® West Femto Maximum Sensitivity Substrate according to the manufacturer's instructions (Pierce, Rockford, IL, USA).

Immunoprecipitation

Nuclear extracts from 293T cells were precleared with 2 µg normal mouse IgG (Santa Cruz Biotechnology, Santa Cruz, CA, USA) and 100 µl slurry of 50% washed Protein A/G Sepharose™ 4 Fast Flow beads (GE Healthcare Bio-Sciences Corporation, Piscataway, NJ, USA) during rotation for 1 h at 4°C in Buffer IPB (10 mM Tris pH 7.4, 100 mM NaCl, 2.5 mM MgCl₂, 0.5% Triton-X) with protease inhibitors (Roche Diagnostics Corporation) as described previously for immunoprecipitation with anti-Sm (8). The beads were discarded and the cleared supernatants were immunoprecipitated with 2 µg anti-Sm or 2 µg IgG for 1 h at 4°C and then bound to 100 µl slurry of 50% washed Protein A/G Sepharose™ 4 Fast Flow beads (GE Healthcare Bio-Sciences Corporation) during rotation for 1 h at 4°C. The immunoprecipitant-bead complexes were washed three times in cold Buffer IPB, then washed and resuspended in phosphate buffered saline (PBS) with protease inhibitors. Sample loading dye was added, and the immunoprecipitants were eluted from the beads by incubation at 100°C for 3 min, vortexed, and loaded along with 5% of the input nuclear extract onto a 15% SDS-polyacrylamide gel and immunoblotted with anti-SCNM1 as described above.

Immunocytofluorescence

The full length wildtype *Scnm1* cDNA described above was cloned into the mammalian expression vector pCMVTnT (Promega Corporation, Madison, WI, USA). Mouse *Luc7L2* cDNA type A lacking exon 8 (aa 10–392 Δ10) was cloned into vectors pCMV-MYC and pEGFP-C2 (Clontech Laboratories Inc.). Mouse full length *U1-70K* cDNA was amplified from C57BL/6J brain RNA and cloned into pCMV-MYC. All clones were sequenced.

293T cells were plated at a density of 15×10^4 cells per well of a 12-well plate onto coverslips coated with polylysine (Sigma-Aldrich). After 24 h the cells were washed three times with PBS, fixed with 4% paraformaldehyde for 5 min, washed three times, blocked for at least 1 h with 10% v/v normal goat serum, 0.05% BSA, 0.1% Triton-X, 0.1 M phosphate buffer (PB), and incubated overnight

at 4°C with antibody. Cells were washed three times for 10 min with 0.1 M PB, and incubated with secondary antibodies for 1 h at room temperature. The cells were washed as above, stained for 4 min with 3 nM 4',6-diamidino-2-phenylindole (DAPI) (Sigma-Aldrich), and washed again. Coverslips were mounted on slides with gel-mount (Biomedica Corporation, Foster City, CA, USA), dried and sealed. The slides were assessed by laser assisted confocal microscopy (Fluoview 500-Olympus Microscope and software, Olympus America Inc., Center Valley, PA), in the University of Michigan Microscope and Image Analysis Laboratory (Director: C. Edwards).

Yeast two-hybrid

Full length wildtype *Scnm1* cDNA was amplified from brain RNA from mouse strain C3HeB/FeJ, cloned into the pLexA vector and transformed into yeast strain L40 (MAT α). A pVP16 random-primed mouse cDNA library from day 9.5 and 10.5 embryos was kindly provided by A. Vojtek and screened by large-scale co-transformation as described (35,36). Interacting transformants were identified by activation of the reporter genes *HIS3* and *LacZ*. *HIS3* activation was assessed by growth on selective media lacking histidine, and β -galactosidase activity was assayed by filter lift (35). 'Strongly positive' clones exhibited β -galactosidase staining within 40 min and good growth in medium lacking histidine and containing 3 mM 3-amino-1,2,4-triazole. Two hundred and forty six strongly positive clones were re-plated for analysis by PCR and restriction digestion.

To isolate DNA, a small portion of each yeast colony was suspended in 10 µl 0.02 M NaOH, vortexed to disperse cells, incubated at 100°C for 5 min, cooled in ice and centrifuged briefly to pellet debris (37). PCR amplification was performed using standard conditions in a 50 µl volume using primers complementary to the pVP16 vector and 2 µl of DNA and an annealing temperature of 60°C. Fifteen microlitres of each amplicon was digested with *Alu1* (New England Biolabs, Boston, MA, USA) for 2 h and then electrophoresed through 2% agarose for 40 min. one to three clones with identical *Alu1* patterns were pooled, sequenced at the University of Michigan Sequencing Core (Director: R. Lyons), and identified by nucleotide–nucleotide Blast search at NCBI (<http://www.ncbi.nlm.nih.gov/>).

Mating assays were performed as previously described (35). The MAT α yeast strain, AMR70, was transformed with LexA-fusion proteins (Fig. 3A) and mated with strain L40 pVP16-y3. Inserts for pVP16 constructs containing mouse *LUC7L2*, *LUC7L* and *CROP* cDNAs were prepared by RT–PCR from C57BL/6J brain RNA.

Northern blot and RT–PCR

RNA was isolated from C57BL/6J mouse tissues using Trizol (Invitrogen Corporation). Poly(A)⁺ RNA was prepared using PolyAtract mRNA isolation System IV (Promega Corporation). Northern blots were prepared as previously described (38,39). The 372 bp *Luc7L2* cDNA coding probe containing exons 9 and 10 (*NM_138680*) was amplified with primers: RS-F: 5'-ATGTCACGAGAACGCAAGAG and RS-R:

5'-GCTCCATGGGAAGCTTAAGGA. The 580 bp probe from the 3'-UTR in exon 10 consisted of two fragments of 294 bp (Ua) and 286 bp (Ub), respectively, amplified with primers 3U-Fa: 5'-AGCTCTGAAGAGCGTGAAGC and 3U-Ra: 5'-AACACAATTCATTCCTACTACTCC; and 3U-Fb: 5'-CACCACCACTGTAACCTGTTGA and 3U-Rb: 5'-TGGTTTTTATTTCAGGCTTGTC. The 455 bp probe from the 3'-UTR in intron 9 (BC056383) was amplified with primers 3U-Fg: 5'-TGGAGTTTTCTGTGTGGGAGA and 3U-Rg: 5'-CCAAGTTCAGGAAGCCTCAG. Probes were amplified from C57BL/6J brain cDNA and labeled by random priming with [α - 32 P]dCTP and [α - 32 P]dATP (GE Healthcare Bio-Sciences Corporation). For RT-PCR of *Luc7L2* from mouse tissues, first strand cDNA was synthesized from 2 μ g of total RNA or 200 ng of poly(A)⁺ RNA using the Superscript First Stand Synthesis System for RT-PCR (Invitrogen Corporation). Amplification was carried out for 28 cycles in a 50 μ l volume with 1 μ l of cDNA. Amplified products were electrophoresed on 2% agarose and visualized by ethidium bromide staining.

Scn8a minigene splicing assay

The 3.6 kb mouse *Scn8a-medJ* minigene construct was cloned by incorporation of three genomic DNA fragments into the vector pCMVtnt. An 0.85 kb fragment containing exon 1 with 67 bp of 5'-UTR and 499 bp of intron 1, flanked by engineered *XhoI* and *KpnI* restriction sites, was amplified from BAC clone 270F06 from strain 129/SvJ (Levin *et al.*, 2004). A 1.35 kb fragment containing exon 2 with 0.6 kb of intron 1 and 0.66 kb of intron 2 with flanking *KpnI* and *SmaI* restriction sites was amplified from the same BAC. A 1.4 kb fragment containing the rest of intron 2 as well as exon 3, intron 3 and exon 4, was amplified from homozygous *Scn8a^{medJ}* DNA containing the mutant splice donor site of exon 3. The last 20 bp of exon 4 were replaced by a 35 bp unique tag. The 1.4 kb fragment was flanked by engineered *SmaI* and *NotI* restriction sites. The minigene construct was sequenced to confirm correct integration of the three fragments.

The minigene construct (0.3 μ g) was transfected with 2 μ g of additional DNA from different combinations of pCMVtnt empty vector, pCMV-SCNM1 and pEGFP-LUC7L2. Three replicate transfections were performed. After 48 h, RNA was extracted using the RNeasy Mini Kit (Qiagen Incorporated, Valencia, CA, USA) with DNase treatment. cDNA was synthesized using oligo-dT and the First Strand Synthesis System (Stratagene, La Jolla, CA, USA). Using a forward primer in exon 1 and reverse FAM-labeled primer in the unique tag of exon 4, the minigene transcript was amplified using 30 cycles. Triplicate PCR reactions were carried out for each cDNA, and the products (1 μ l) were analyzed on an ABI 3730 sequencer (Applied Biosystems, Foster City, CA, USA). The area under the peaks was quantitated using Applied Biosystems Genemapper v3.7 software by the University of Michigan Sequencing Core (B. Lyons, Director).

ACKNOWLEDGEMENTS

We thank Anne Vojtek for generously providing plasmids pLexA and pVP16 and the mouse embryonic cDNA library as well as valuable technical advice. We thank Joan Steitz for the gift of Sm antiserum, and Michelle Trudeau for assistance with cloning the HIS-SCNM1 construct. 'Funding to pay Open Access publication Charges for this article was provided by The University of Michigan.'

Conflict of Interest statement. None declared.

FUNDING

National Institutes of Health (R01 GM24872 to M.H.M.); National Health and Medical Research Council of Australia (CJ Martin Research Fellowship 358774 to V.M.H.)

REFERENCES

- Buchner, D.A., Trudeau, M. and Meisler, M.H. (2003) SCNM1, a putative RNA splicing factor that modifies disease severity in mice. *Science*, **301**, 967–969.
- Kearney, J.A., Buchner, D.A., De Haan, G., Adamska, M., Levin, S.I., Furay, A.R., Albin, R.L., Jones, J.M., Montal, M., Stevens, M.J. *et al.* (2002) Molecular and pathological effects of a modifier gene on deficiency of the sodium channel *Scn8a* (Na(v)1.6). *Hum. Mol. Genet.*, **11**, 2765–2775.
- Jurica, M.S. and Moore, M.J. (2003) Pre-mRNA splicing: awash in a sea of proteins. *Mol. Cell*, **12**, 5–14.
- Lerner, E.A., Lerner, M.R., Janeway, C.A., Jr. and Steitz, J.A. (1981) Monoclonal antibodies to nucleic acid-containing cellular constituents: probes for molecular biology and autoimmune disease. *Proc. Natl Acad. Sci. USA*, **78**, 2737–2741.
- Cao, W. and Garcia-Blanco, M.A. (1998) A serine/arginine-rich domain in the human U1 70 k protein is necessary and sufficient for ASF/SF2 binding. *J. Biol. Chem.*, **273**, 20629–20635.
- Carrero, G., Hendzel, M.J. and de Vries, G. (2006) Modelling the compartmentalization of splicing factors. *J. Theor. Biol.*, **239**, 298–312.
- Lamond, A.I. and Spector, D.L. (2003) Nuclear speckles: a model for nuclear organelles. *Nat. Rev. Mol. Cell. Biol.*, **4**, 605–612.
- Charroux, B., Pellizzoni, L., Perkinson, R.A., Shevchenko, A., Mann, M. and Dreyfuss, G. (1999) Gemin3: A novel DEAD box protein that interacts with SMN, the spinal muscular atrophy gene product, and is a component of gems. *J. Cell. Biol.*, **147**, 1181–1194.
- Hoet, R.M., Raats, J.M., de Wildt, R., Dumortier, H., Muller, S., van den Hoogen, F. and van Venrooij, W.J. (1998) Human monoclonal autoantibody fragments from combinatorial antibody libraries directed to the U1snRNP associated UIC protein; epitope mapping, immunolocalization and V-gene usage. *Mol. Immunol.*, **35**, 1045–1055.
- Stanek, D. and Neugebauer, K.M. (2006) The Cajal body: a meeting place for spliceosomal snRNPs in the nuclear maze. *Chromosoma*, **115**, 343–354.
- Fortes, P., Bilbao-Cortes, D., Fornerod, M., Rigaut, G., Raymond, W., Seraphin, B. and Mattaj, I.W. (1999) Luc7p, a novel yeast U1 snRNP protein with a role in 5' splice site recognition. *Genes Dev.*, **13**, 2425–2438.
- Brahms, H., Raymackers, J., Union, A., de Keyser, F., Meheus, L. and Luhrmann, R. (2000) The C-terminal RG dipeptide repeats of the spliceosomal Sm proteins D1 and D3 contain symmetrical dimethylarginines, which form a major B-cell epitope for anti-Sm autoantibodies. *J. Biol. Chem.*, **275**, 17122–17129.
- Kohman, D.C., Harris, J.B. and Meisler, M.H. (1996) Mutation detection in the *med* and *medJ* alleles of the sodium channel *Scn8a*: unusual patterns of exon splicing are influenced by a minor class AT–AC intron. *J. Biol. Chem.*, **271**, 17576–17581.
- Kimura, E., Hidaka, K., Kida, Y., Morisaki, H., Shirai, M., Araki, K., Suzuki, M., Yamamura, K.I. and Morisaki, T. (2004) Serine-arginine-rich nuclear protein Luc7l regulates myogenesis in mice. *Gene*, **341**, 41–47.

15. Umehara, H., Nishii, Y., Morishima, M., Kakehi, Y., Kioka, N., Amachi, T., Koizumi, J., Hagiwara, M. and Ueda, K. (2003) Effect of cisplatin treatment on speckled distribution of a serine/arginine-rich nuclear protein CROP/Luc7A. *Biochem. Biophys. Res. Commun.*, **301**, 324–329.
16. Hedley, M.L., Amrein, H. and Maniatis, T. (1995) An amino acid sequence motif sufficient for subnuclear localization of an arginine/serine-rich splicing factor. *Proc. Natl Acad. Sci. USA*, **92**, 11524–11528.
17. Forch, P., Puig, O., Martinez, C., Seraphin, B. and Valcarcel, J. (2002) The splicing regulator TIA-1 interacts with U1-C to promote U1 snRNP recruitment to 5' splice sites. *Embo J.*, **21**, 6882–6892.
18. Nelissen, R.L., Will, C.L., van Venrooij, W.J. and Luhrmann, R. (1994) The association of the U1-specific 70 K and C proteins with U1 snRNPs is mediated in part by common U snRNP proteins. *Embo J.*, **13**, 4113–4125.
19. Du, H. and Rosbash, M. (2002) The U1 snRNP protein U1C recognizes the 5' splice site in the absence of base pairing. *Nature*, **419**, 86–90.
20. Tardiff, D.F. and Rosbash, M. (2006) Arrested yeast splicing complexes indicate stepwise snRNP recruitment during *in vivo* spliceosome assembly. *RNA*, **12**, 968–979.
21. Fortes, P., Kufel, J., Fornerod, M., Polycarpou-Schwarz, M., Lafontaine, D., Tollervey, D. and Mattaj, I.W. (1999) Genetic and physical interactions involving the yeast nuclear cap-binding complex. *Mol. Cell. Biol.*, **19**, 6543–6553.
22. Philipps, D., Celotto, A.M., Wang, Q.Q., Tarng, R.S. and Graveley, B.R. (2003) Arginine/serine repeats are sufficient to constitute a splicing activation domain. *Nucleic Acids Res.*, **31**, 6502–6508.
23. Gavin, A.C., Bosche, M., Krause, R., Grandi, P., Marzioch, M., Bauer, A., Schultz, J., Rick, J.M., Michon, A.M., Cruciat, C.M. *et al.* (2002) Functional organization of the yeast proteome by systematic analysis of protein complexes. *Nature*, **415**, 141–147.
24. Zhou, Z., Licklider, L.J., Gygi, S.P. and Reed, R. (2002) Comprehensive proteomic analysis of the human spliceosome. *Nature*, **419**, 182–185.
25. Cazalla, D., Newton, K. and Caceres, J.F. (2005) A novel SR-related protein is required for the second step of Pre-mRNA splicing. *Mol. Cell. Biol.*, **25**, 2969–2980.
26. Shipman, K.L., Robinson, P.J., King, B.R., Smith, R. and Nicholson, R.C. (2006) Identification of a family of DNA-binding proteins with homology to RNA splicing factors. *Biochem. Cell. Biol.*, **84**, 9–19.
27. Slaugenhaupt, S.A., Blumenfeld, A., Gill, S.P., Leyne, M., Mull, J., Cuajungco, M.P., Liebert, C.B., Chadwick, B., Idelson, M., Reznik, L. *et al.* (2001) Tissue-specific expression of a splicing mutation in the IKBKAP gene causes familial dysautonomia. *Am. J. Hum. Genet.*, **68**, 598–605.
28. Nissim-Rafinia, M. and Kerem, B. (2002) Splicing regulation as a potential genetic modifier. *Trends Genet.*, **18**, 123–127.
29. Chang, J.G., Hsieh-Li, H.M., Jong, Y.J., Wang, N.M., Tsai, C.H. and Li, H. (2001) Treatment of spinal muscular atrophy by sodium butyrate. *Proc. Natl Acad. Sci. USA*, **98**, 9808–9813.
30. Hims, M.M., Ibrahim el, C., Leyne, M., Mull, J., Liu, L., Lazaro, C., Shetty, R.S., Gill, S., Gusella, J.F., Reed, R. *et al.* (2007) Therapeutic potential and mechanism of kintin as a treatment for the human splicing disease familial dysautonomia. *J. Mol. Med.*, **85**, 149–161.
31. Nissim-Rafinia, M., Aviram, M., Randell, S.H., Shushi, L., Ozeri, E., Chiba-Falek, O., Eidelman, O., Pollard, H.B., Yankaskas, J.R. and Kerem, B. (2004) Restoration of the cystic fibrosis transmembrane conductance regulator function by splicing modulation. *EMBO Rep.*, **5**, 1071–1077.
32. Ayala, Y.M., Pagani, F. and Baralle, F.E. (2006) TDP43 depletion rescues aberrant CFTR exon 9 skipping. *FEBS Lett.*, **580**, 1339–1344.
33. Yang, Y. and Walsh, C.E. (2005) Spliceosome-mediated RNA trans-splicing. *Mol. Ther.*, **12**, 1006–1012.
34. Kastner, B., Kornstadt, U., Bach, M. and Luhrmann, R. (1992) Structure of the small nuclear RNP particle U1: identification of the two structural protuberances with RNP-antigens A and 70 K. *J. Cell. Biol.*, **116**, 839–849.
35. Vojtek, A.B., Hollenberg, S.M. and Cooper, J.A. (1993) Mammalian Ras interacts directly with the serine/threonine kinase Raf. *Cell*, **74**, 205–214.
36. Hollenberg, S.M., Sternglanz, R., Cheng, P.F. and Weintraub, H. (1995) Identification of a new family of tissue-specific basic helix–loop–helix proteins with a two-hybrid system. *Mol. Cell. Biol.*, **15**, 3813–3822.
37. Fromont-Racine, M., Rain, J.C. and Legrain, P. (2002) Building protein–protein networks by two-hybrid mating strategy. *Methods Enzymol.*, **350**, 513–524.
38. Kearney, J.A., Plummer, N.W., Smith, M.R., Kapur, J., Cummins, T.R., Waxman, S.G., Goldin, A.L. and Meisler, M.H. (2001) A gain-of-function mutation in the sodium channel gene Scn2a results in seizures and behavioral abnormalities. *Neuroscience*, **102**, 307–317.
39. Buchner, D.A. and Meisler, M.H. (2003) TSRC1, a widely expressed gene containing seven thrombospondin type 1 repeats. *Gene*, **307**, 23–30.
40. Muto, Y., Pomeranz Krummel, D., Oubridge, C., Hernandez, H., Robinson, C.V., Neuhaus, D. and Nagai, K. (2004) The structure and biochemical properties of the human spliceosomal protein U1C. *J. Mol. Biol.*, **341**, 185–198.
41. Levin, S.I. and Meisler, M.H. (2004) Floxed allele for conditional inactivation of the voltage-gated sodium channel Scn8a (NaV1.6). *Genesis*, **39**, 234–239.